The EMBO Journal (2013) 32, 245–259
www.embojournal.org

SOURCE DATA | TRANSPARENT PROCESS

THE EMBO JOURNAL

Drosophila ATP6AP2/VhaPRR functions both as a novel planar cell polarity core protein and a regulator of endosomal trafficking

Tobias Hermle[1,2,5,*], Maria Clara Guida[1,2,3,5], Samuel Beck[1,2], Susanne Helmstädter[1,2] and Matias Simons[1,2,4,*]

[1]Center for Systems Biology (ZBSA), University of Freiburg, Freiburg, Germany, [2]Renal Division, University Hospital Freiburg, Freiburg, Germany, [3]Graduate Program GRK1104, University of Freiburg, Freiburg, Germany and [4]BIOSS Centre for Biological Signalling Studies, University of Freiburg, Freiburg, Germany

Planar cell polarity (PCP) controls the orientation of cells within tissues and the polarized outgrowth of cellular appendages. So far, six PCP core proteins including the transmembrane proteins Frizzled (Fz), Strabismus (Stbm) and Flamingo (Fmi) have been identified. These proteins form asymmetric PCP domains at apical junctions of epithelial cells. Here, we demonstrate that VhaPRR, an accessory subunit of the proton pump V-ATPase, directly interacts with the protocadherin Fmi through its extracellular domain. It also shows a striking co-localization with PCP proteins during all pupal wing stages in *Drosophila*. This localization depends on intact PCP domains. Reversely, VhaPRR is required for stable PCP domains, identifying it as a novel PCP core protein. VhaPRR performs an additional role in vesicular acidification as well as endolysosomal sorting and degradation. Membrane proteins, such as E-Cadherin and the Notch receptor, accumulate at the surface and in intracellular vesicles of cells mutant for *VhaPRR*. This trafficking defect is shared by other V-ATPase subunits. By contrast, the V-ATPase does not seem to have a direct role in PCP regulation. Together, our results suggest two roles for VhaPRR, one for PCP and another in endosomal trafficking. This dual function establishes VhaPRR as a key factor in epithelial morphogenesis.

The EMBO Journal (2013) **32,** 245–259. doi:10.1038/emboj.2012.323; Published online 4 January 2013
Subject Categories: membranes & transport; development
Keywords: E-Cadherin; endosomal trafficking; epithelial polarity; lysosomes; planar cell polarity

*Corresponding authors. M Simons, Center for Systems Biology (ZBSA)/Renal Division, University Hospital Freiburg, Habsburgerstr. 49, 79104 Freiburg, Germany. Tel.: +49 761 20397206; Fax: +49 761 20397188; E-mail: matias.simons@uniklinik-freiburg.de or T Hermle, Renal Division, University Hospital Freiburg, Habsburgerstr. 55, 79104 Freiburg, Germany. Tel.: +49 761 20397210; Fax: +49 761 20397188; E-mail: tobias.hermle@uniklinik-freiburg.de
[5]These two authors contributed equally to this work

Received: 31 May 2012; accepted: 7 November 2012; published online: 4 January 2013

Introduction

The planar cell polarity (PCP) pathway is a highly conserved pathway that polarizes cells in the plane of a tissue and equips cells with a defined orientation. In *Drosophila*, PCP is evident in the organization of cuticular structures, such as wing hair or body bristles, and in the orientation of photoreceptor clusters of the eye. In vertebrates, the coordinated beating of cilia and the directional cell migration during gastrulation or epidermal wound healing are examples of important processes that rely on PCP (Simons and Mlodzik, 2008; Bayly and Axelrod, 2011; Goodrich and Strutt, 2011). As a consequence, defective PCP signalling contributes to many diseases including tissue fusion disorders (e.g., neural tube defects) and ciliopathies (e.g., polycystic kidney disease; Simons and Walz, 2006). On the molecular level, there are two conserved PCP protein cassettes: the Fat/Dachsous group and the classical PCP core group consisting of Frizzled (Fz), Dishevelled (Dsh), Flamingo/Starry night (Fmi/Stan), Strabismus/Van Gogh (Stbm/Vang), Prickle and Diego. Fz and Dsh also function in the Wingless (Wg) or canonical Wnt pathway (Veeman *et al*, 2003).

An excellent system to study epithelial PCP is the pupal wing epidermis of *Drosophila*. Genetic approaches in pupal wings have uncovered several key features of PCP, including the asymmetric localization of the PCP complex. It was shown that Fz and Dsh localize to the distal plasma membrane, whereas Stbm and Pk localize to the proximal membrane (Axelrod, 2001; Strutt, 2001; Bastock *et al*, 2003). The protocadherin Fmi shows homophilic-binding behaviour and localizes to both membranes (Usui *et al*, 1999). It has also become clear that these PCP domains are already formed in larval stages and are temporarily lost during a phase of junctional remodelling in pupal wing morphogenesis (Aigouy *et al*, 2010).

Recent evidence suggests that the formation of the complex requires polarized transport of PCP proteins to the proximal–distal (P–D) boundaries along microtubules (Shimada *et al*, 2006). The maintenance of the complex involves rapid turnover of non-complexed components by endocytosis and recycling (Shimada *et al*, 2006; Strutt *et al*, 2011). These dynamic membrane trafficking events seem to involve the recruitment of components of the endocytic machinery by Fmi (Classen *et al*, 2005; Mottola *et al*, 2010). However, the underlying mechanisms remain poorly understood.

We and others recently demonstrated that an accessory subunit of the vacuolar (V)-ATPase, VhaPRR (also called PRR or ATP6AP2 in mammals), plays a role in both canonical Wnt and PCP signalling (Buechling *et al*, 2010; Cruciat *et al*, 2010; Hermle *et al*, 2010). The V-ATPase is a large protein complex consisting of a peripheral V1 domain with eight subunits for ATP hydrolysis, and a V0 domain with six subunits for proton translocation (Forgac, 2007). Many of these subunits are expressed in different isoforms and splice variants, further

increasing the complexity of the V-ATPase. The two accessory subunits (ATP6AP1/Ac45 and ATP6AP2/PRR) are not found in unicellular organisms, suggesting that they are not essential for proton pump activity. The V-ATPase acidifies intracellular organelles and the extracellular space depending on its subcellular localization. One prominent function of the V-ATPase is to ensure a low intraluminal pH required for protein degradation by lysosomal hydrolases. Additional functions of the V-ATPase in signalling, membrane trafficking and the regulation of post-translational modifications of proteins have also been proposed (Forgac, 2007; Sihn *et al*, 2010).

During an effort to purify the V-ATPase complex from adrenal chromaffin cells, VhaPRR was discovered as an 8.9-kDa fragment containing the transmembrane domain and the cytosolic tail (Ludwig *et al*, 1998). Later, the full-length protein (37 kDa) was cloned as a receptor for (pro)renin (PRR; Nguyen *et al*, 2002). The *Drosophila* name for ATP6AP2/PRR, VhaPRR, reflects the proposed dual function of the mammalian protein. Previous studies demonstrated that ATP6AP2/PRR undergoes proteolytic cleavage generating the 8.9-kDa-transmembrane stump and a 28-kDa-sized N-terminal soluble fragment (sPRR) that can be detected in urine and plasma samples (Cousin *et al*, 2009). The significance of this cleavage event remains unknown. Moreover, tissue-specific conditional knockout approaches have revealed important functions of ATP6AP2/PRR in the survival of murine cardiomyocytes and podocytes (Kinouchi *et al*, 2010; Oshima *et al*, 2011; Riediger *et al*, 2011). The only described human ATP6AP2/PRR mutation so far is a hypomorphic mutation that results in mental retardation and epilepsy in the affected individuals (Ramser *et al*, 2005).

In the context of Wnt signalling, ATP6AP2/PRR was shown to function as an adaptor between the V-ATPase and Fz in acidic endosomal compartments. The Fz-V-ATPase clusters also contained activated forms of the Wnt co-receptor LRP6, thus, promoting Wnt signalling (Cruciat *et al*, 2010). Similarly, knockdown of VhaPRR in the *Drosophila* wing led to defects in both Wg and PCP signalling. VhaPRR was shown to interact genetically and physically with Fz, and the absence of VhaPRR caused mislocalization of Fz in pupal wing cells (Buechling *et al*, 2010; Hermle *et al*, 2010). However, lack of VhaPRR also generated other phenotypes, including vein alterations and bristle duplications, suggestive of additional unknown functions.

Here, we use genetics and biochemistry in a well-characterized PCP system to demonstrate that VhaPRR fulfills all criteria of a PCP core protein. In addition, we show that VhaPRR acts as a regulator of endosomal sorting and protein degradation. Our findings suggest that VhaPRR is an important regulator of epithelial morphogenesis.

Results

VhaPRR is required for PCP core protein localization

To characterize the role of VhaPRR in PCP in more detail, we generated a mutant allele by imprecise P-element excision. The excision deleted 860 bp of the *VhaPRR* locus including the first two of the three exons (Supplementary Figure S1A), containing the epitope sequence of our antibody (see below). The specificity of the allele ($VhaPRR^{\Delta 1}$) was determined by introducing one copy of a genomic construct harbouring the entire 2.6 kb-genomic locus. The rescue construct restored viability producing adult flies without obvious phenotypes. Consistent with previous RNAi experiments (Buechling *et al*, 2010; Hermle *et al*, 2010), clonal elimination of *VhaPRR* in the pupal wing led to a significant delay in prehair formation and, occasionally, multiple wing hairs emerging from one cell (Figure 1A and B). In the adult wing and notum, *VhaPRR* clones showed hair and bristle polarity defects, respectively (Supplementary Figure S1D and E). Generally, PCP phenotypes were stronger in pupal than in adult stages. In the adult leg, lack of VhaPRR caused a mispatterning of tarsal segments similar to phenotypes previously observed for *PCP* mutants (Supplementary Figure S1F and G; Gubb *et al*, 1999; Lee and Adler, 2002). In addition to the PCP phenotypes, the clones also displayed signs of impaired Notch signalling including ectopic notum bristles and vein thickening and loss (Supplementary Figure S1B–E; Dietzl *et al*, 2007).

Immunostaining of PCP core proteins revealed the following changes inside the mutant clone: both Fz and Stbm were reduced at apical junctions. In addition, both proteins showed a partial overlap in vesicular compartments (Figure 1C, D and F). Fmi also lost its ability to maintain an asymmetric localization and showed a slight cytoplasmic increase inside the clone (Figure 1E). All effects were slightly stronger than those achieved with RNAi knockdown (Hermle *et al*, 2010), suggesting a more complete elimination of expression with the mutant (also see below in section on acidification).

Because these findings indicated that lack of VhaPRR reduces the integrity of the PCP complex, we next attempted to test the stability of the PCP domains using a Fmi antibody internalization assay (Strutt *et al*, 2011). This experiment is performed in the prepupal wing (around 5 h APF), because at this developmental stage there is no cuticle yet, which allows the application of an antibody. PCP domains do exist at this stage, but they are less coherent and point towards the wing margin (Figure 1G and H; Classen *et al*, 2005; Aigouy *et al*, 2010). For the uptake assay, live prepupal wings were dissected, and incubated at 4°C with an antibody against Fmi, followed by chasing at 29°C for 45 min before fixation (Strutt *et al*, 2011). We detected a stronger reduction of Fmi at the apical junctions of *VhaPRR* mutant clones compared with the neighbouring wild-type cells, reflecting an increased Fmi internalization inside the clones (Figure 1H). The difference between the mutant and wild-type tissue was much less pronounced when the chase was carried out at 4°C, a temperature that strongly attenuates endocytosis (Figure 1G and I). Collectively, these results suggest that VhaPRR functions in PCP by stabilizing asymmetric PCP domains.

VhaPRR localizes to PCP domains

To study the localization of VhaPRR in the pupal wing cells, we raised an antibody against VhaPRR. The antibody was directed against the extracellular domain potentially recognizing both uncleaved VhaPRR and sPRR. Antibody specificity was confirmed by western blot analysis of *VhaPRR* RNAi-treated S2 cells as well as by staining of mutant clones (Figures 2D and 4D).

In immunostainings of pupal wings, we found that VhaPRR co-localized with the PCP domains at all stages of pupal development: in prepupal stages, VhaPRR was polarized towards the wing margin (Figure 2A); during the junctional

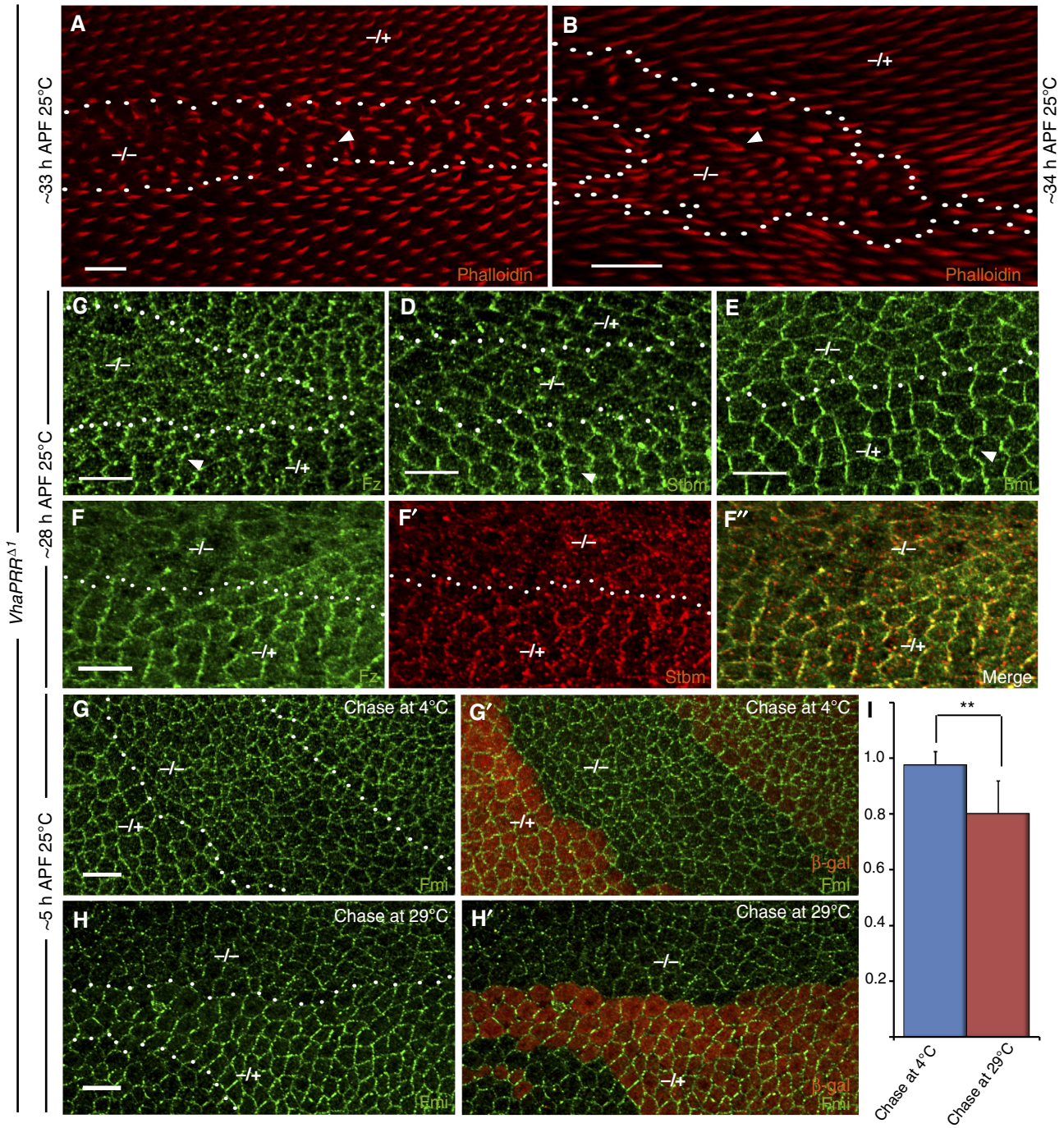

Figure 1 Loss of VhaPRR causes PCP defects and PCP core protein mislocalization. All clones are marked by loss of β-galactosidase (β-gal; only shown in (**F**′, **G**′) in red). Clone outlines are marked with a dotted white line. In all figures, mutant homozygous areas are marked with '−/−', and heterozygous areas with '−/+'. Cells in the latter areas are the control cells. Scale bars represent 10 μm in all figures, unless otherwise stated. The proximal side of the wing is to the left, the distal to the right. Anterior is up, posterior is down. (**A**, **B**) Prehairs inside and outside, the *VhaPRR* mutant clone are stained with Phalloidin (red). In addition to the wing hair mispolarization, more than one hair per cell is occasionally observed (arrowheads). Hairs are shorter, thus showing a significant delay in prehair formation. Phenotypes are usually weaker at later stages ((**B**) is slightly later as can be seen by the longer hairs; for adult wings see Supplementary Figure S1). (**C**, **D**) Fz (**C**) and Stbm (**D**; both green) are mislocalized inside *VhaPRR* mutant clones. Arrowheads mark normal asymmetric localization in control tissue. (**E**) Fmi (green) is less asymmetric and also shows a diffusely enhanced cytoplasmic staining. (**F**, **F**′, **F**″) Fz and Stbm show partial overlap in residual PCP domains and intracellular vesicles. (**G**–**I**) Fmi antibody uptake assay in live prepupal wings. At this developmental stage, PCP domains point towards the wing margin and are less organized than at 28 h APF. (**G**) Fmi localization inside *VhaPRR* clones is comparable to wild-type tissue, when the chase after Fmi antibody binding is performed at 4°C, which attenuates endocytosis. Note that effects on Fmi localization caused by removal of VhaPRR become apparent at later stages (see above). (**H**, **H**′) A 45-min chase at 29°C causes a reduction of Fmi at apical junctions inside *VhaPRR* mutant clones, reflecting increased internalization of Fmi in the absence of VhaPRR compared with the neighbouring wild-type tissue. (**I**) Quantification of antibody uptake experiment. Average staining intensity of mutant and the surrounding wild-type tissue was measured as a ratio in shown in the *y* axis. When endocytic activity is abrogated at 4°C, the ratio is slightly below 1.0. Error bars represent standard error of the mean, and statistical significance was determined using unpaired Student's *t*-test (**$P<0.01$).

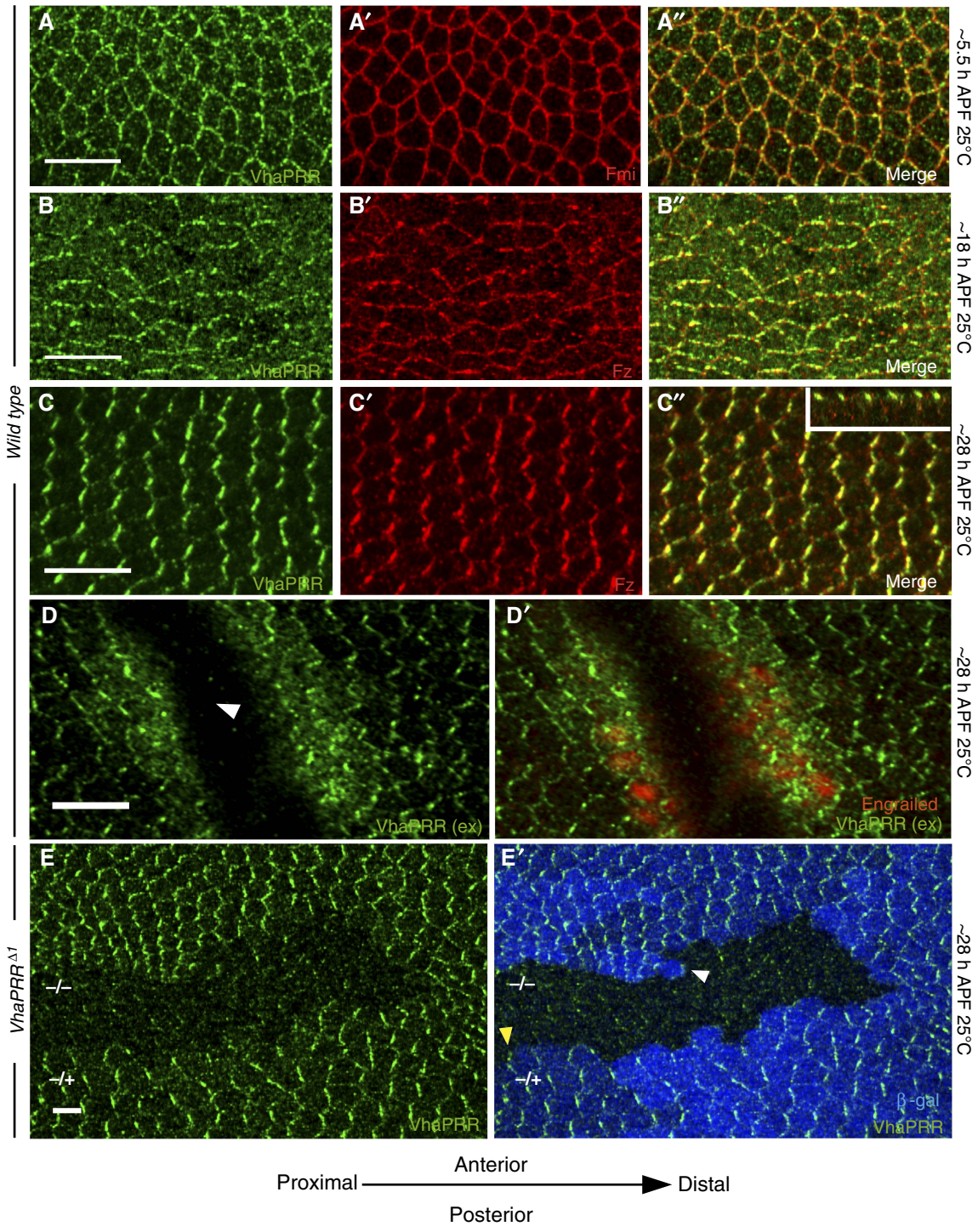

Figure 2 VhaPRR localizes to PCP domains. (**A**–**E**) Immunostainings of pupal wings from different developmental stages are shown. (**A, A′, A″**) VhaPRR (green) co-localizes with Fmi (red) in prepupal wings (5.5 h APF). At this stage, PCP domains point towards the wing margin. (**B**) At 18 h APF, VhaPRR localization is more irregular. Junctional staining is still visible, but also intracellular staining, reflecting the dynamic cell rearrangements during this phase (Aigouy *et al*, 2010). Co-localization with Fz (**B′**; red) is shown in (**B″**). (**C**) VhaPRR shows maximal asymmetric localization beyond 28 h APF. Co-localization with Fz (**C′**) is shown in (**C″**). The *x*–*z* projection in the inset of (**C″**) shows co-localization of VhaPRR and Fz at apical junctions. (**D**) VhaPRR staining without permeabilization shows that the junctional pool is at the surface. The fine vesicular staining usually observed by staining with detergent is strongly decreased with this technique. Interestingly, at sites where the pupal wing tissue has been injured with the forceps during dissection (arrowhead), an additional intracellular pool becomes apparent. In the wound egde cells another intracellular antigen, Engrailed, can also be detected (**D′**). Engrailed is not detected in cells away from the wound, demonstrating the efficiency of both the surface staining and the wounding. (**E, E′**) VhaPRR is lost from *VhaPRR*$^{\Delta 1}$ mutant clones at 28 h. Clones are marked by loss of β-gal (in blue). Note that also the cytoplasmic staining of VhaPRR is slightly reduced inside the clone. Arrowheads in (**D′**) show that VhaPRR can localize to proximal (yellow) and distal (white) clone boundaries (scale bar 5 μm).

remodelling phase (Aigouy *et al*, 2010), the protein partly relocalized to intracellular compartments (Figure 2B); and before prehair formation, the enrichment at P–D membranes reached its maximum (Figure 2C): VhaPRR concentrated with the other PCP core proteins at P–D boundaries and spared anterior–posterior (A–P) boundaries. By performing the staining without permeabilization, we confirmed that this pattern reflects the cell surface pool of VhaPRR (Figure 2D). However, in this experiment we also noted that at sites where the pupal wing epithelium had been injured with the forceps, the antibody was able to bind to an additional intracellular pool of VhaPRR (Figure 3D′). At *VhaPRR* clone boundaries, VhaPRR appears to localize to both proximal and distal sides of wild-type cells facing the clone (Figure 2D).

VhaPRR localization and stability is controlled by Fmi

Next, we asked whether the association of VhaPRR with the polarized PCP domains depends on PCP proteins. For this, we induced *fz* mutant clones and expressed *Fmi* and *Stbm* RNAi in *flp*-out clones, respectively. In all cases, VhaPRR levels were strongly reduced inside the clones (Figure 3A–C). At clone boundaries, VhaPRR recapitulated the typical localization of PCP transmembrane core proteins (Strutt, 2001; Strutt and Strutt, 2008): whereas in *fz* and *Stbm* RNAi clones VhaPRR was still present at clone boundaries, it was completely lost at boundaries of *Fmi* RNAi clones (Figure 3A–C).

By contrast, we detected a striking stabilization of VhaPRR in Fmi overexpression clones or other GAL4-controlled expression domains (Figure 3D). VhaPRR accumulated together with Fmi at apical junctions and Hrs-positive subapical vesicles, suggesting that the complex shuttles between the plasma membrane and endosomes (Figure 3D′). *In situ* hybridization showed no increase of *VhaPRR* expression, indicating that VhaPRR gain was not caused by increased gene expression (Supplementary Figure S2).

The opposite result—a severe destabilization of VhaPRR—was found inside Fz and Stbm overexpression clones (Figure 3E and F). In addition, VhaPRR was enriched at the boundaries of Fz overexpression clones and at non-autonomously reoriented PCP domains surrounding the clones (Figure 3E and E′). The overexpression of Fz with *patched(ptc)*-GAL4 displaced Fmi from apical junctions into the cytoplasm (Figure 3G), suggesting that VhaPRR loss inside the Fz overexpression clone could be secondary to the reduction of junctional Fmi and/or the masking of VhaPRR-binding sites on Fmi. This is supported by the co-expression of Fz and Fmi (Figure 3H). Here, VhaPRR was stabilized to a similar degree as by the single expression of Fmi, suggesting that Fmi effects are dominant over Fz effects (Figure 3H). Together, these results propose that VhaPRR requires intact PCP domains for its junctional localization. Moreover, recruitment of VhaPRR to the domains appears to depend on Fmi.

The extracellular part of VhaPRR is secreted and binds to Fmi

We further discovered that the simultaneous overexpression of Fmi and *VhaPRR* RNAi in the *ptc* or *engrailed* domain of the pupal wing displayed an accumulation of VhaPRR. This means that, despite the knockdown, VhaPRR was increased within the Fmi expression area (Figure 4A). Furthermore, beyond 33–34 h APF VhaPRR partially reappeared at the apical junctions within the clones (Figure 4B). The most plausible explanation for these observations is that the reported extracellular cleavage product, sPRR, can be secreted and travel extracellularly.

To test whether Fmi could function as a receptor for sPRR, we generated medium conditioned with sPRR. This was achieved either by overexpressing HA-tagged sPRR or by overexpressing full-length VhaPRR in S2 cells (Figure 4C–E). When sPRR–HA conditioned medium was applied onto S2 cells transfected with a Fmi construct, sPRR–HA predominantly bound to cells positive for Fmi and not to non-transfected cells or to cells overexpressing a control transmembrane protein (Figure 5A and B). We also explored whether ectopic sPRR had any effects on PCP signalling *in vivo* by overexpressing sPRR–HA with *ptc*-GAL4. sPRR–HA co-localized with Fmi and Hrs in large subapical vesicles outside of the expression domain (Supplementary Figure S3B), suggesting that the complex of Fmi and sPRR–HA is endocytosed.

Nevertheless, ectopic sPRR was never found at the PCP domains and also did not cause any adult PCP phenotypes (Supplementary Figure S3B and not shown). Similarly, the overexpression of full-length VhaPRR was unable to localize to any cell surface region including the PCP domains. Instead, it was diffusely distributed in the cytoplasm (Supplementary Figure S3C). Together, the results indicate that both endogenous and exogenous sPRR can be secreted in a paracrine manner in the pupal wing epithelium. However, only endogenous sPRR seems to be able to interact with PCP domains.

The cleavage site is not required for PCP signalling and survival

To study the significance of VhaPRR cleavage, we introduced two arginine-to-alanine conversions into the previously characterized consensus motif (RxxR) for cleavage by the protease furin (Figure 4C; Cousin *et al*, 2009). We confirmed in S2 cells and pupae that the exogenous VhaPRR-AxxA is not able to generate sPRR (Supplementary Figure S3D and E). When the same mutations were made in our genomic rescue construct, the resulting rescue flies were indistinguishable from wild-type flies. Viability was not reduced, nor did we see PCP defects or other phenotypes in the adult animals. Furthermore, the mutant and wild-type protein showed a normal junctional localization (Supplementary Figure S3F and not shown). Therefore, it can be concluded that the RxxR cleavage site, which at least for overexpressed VhaPRR is required for sPRR generation, is dispensable for PCP signalling or viability *in vivo*. If no other functional cleavage sites exist, then the full-length form of VhaPRR would be sufficient for proper PCP signalling, despite the binding of endogenous sPRR to PCP domains.

VhaPRR and Fmi physically interact via their extracellular domains

Having shown that VhaPRR requires its extracellular domain for the binding to Fmi, we next tested the structural requirements of Fmi for this interaction. By overexpressing N-terminally and C-terminally truncated versions of Fmi in pupal wings, we could show that most of the extracellular domain including the Cadherin, Laminin G and EGF repeats as well as the whole cytoplasmic tail are dispensable for VhaPRR recruitment and stabilization (Figure 5D and E). The

VhaPRR-interacting domain of Fmi should therefore include the membrane-proximal region (containing the hormone-receptor domain (HRM)) and/or extracellular loops of the transmembrane part.

Finally, to obtain biochemical proof for the interaction between VhaPRR and Fmi, we performed co-immunoprecipitation experiments. Sufficient expression levels could only be obtained in transfected HEK293T cells using mouse versions of Fmi (Celsr-1 and -2) and PRR from *Xenopus laevis*. In these cells, we observed that immunoprecipitation of Celsr-1 and -2–EGFP bound PRR, whereas antibodies against PRR–V5 retained Celsr-1 and -2 (Figure 5F and G).

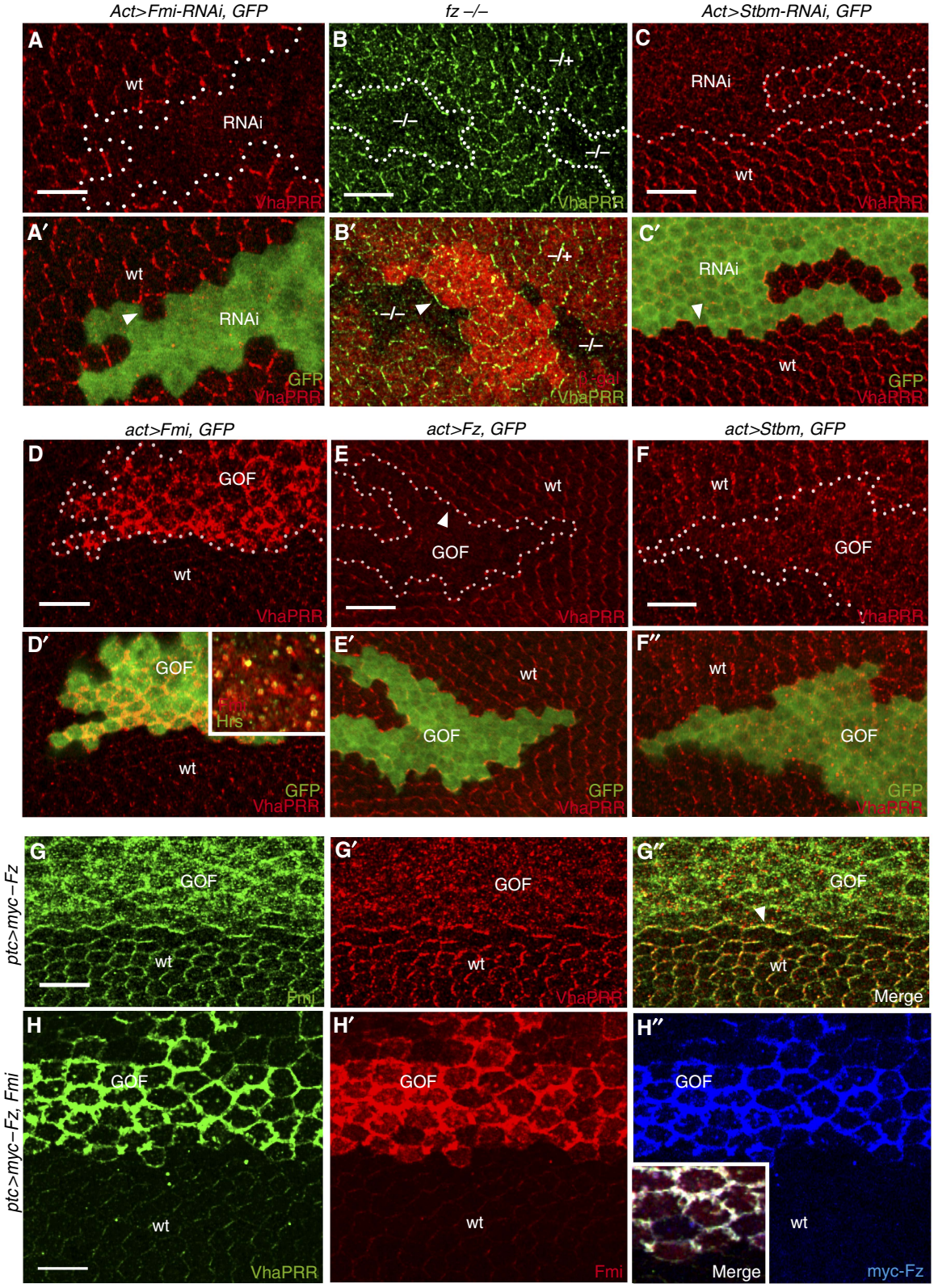

Altogether, these results suggest that VhaPRR possesses all the features of a *bona fide* PCP core protein, including a physical interaction with the PCP complex mediated by Fmi.

VhaPRR participates in vesicular acidification and endolysosomal degradation

One striking difference to mutations in the PCP core proteins was that the lack of VhaPRR caused a significant impairment of cell viability in the pupal wing. $VhaPRR^{\Delta 1}$ clones often contained cleaved Caspase 3 (Cas3)-positive cells (Supplementary Figure S4A). This is an uncommon property of PCP proteins, indicating an additional function crucial for cell survival. Given its association with the V-ATPase complex, lack of VhaPRR might compromise proton transport across cellular membranes and, eventually, cell viability.

Therefore, we first tested the role of VhaPRR in vesicular acidification. We applied the acidotrophic dye Lysotracker to prepupal wings. Whereas VhaPRR RNAi was not sufficient to visibly affect acidification (not shown), *VhaPRR* mutant clones showed an effect on acidification and also on the distribution of acidified vesicles. Lysotracker uptake was reduced in apical parts of the epithelial cells, but appeared normal in more basal parts (Figure 6A and B and inset in B). To ensure that vesicular Lysotracker trapping was a result of V-ATPase activity, we applied the V-ATPase inhibitor Concanamycin A before Lysotracker incubation. This treatment caused the abolishment of all Lysotracker-positive vesicles in apical and basal aspects of mutant and wild-type cells (Figure 6C and D). VhaPRR, thus, appears to have a regulatory function in the acidification of specific apical vesicle populations, but does not seem to be an essential prerequisite for all V-ATPase-mediated proton transport.

To test whether this acidification defect affected endolysosomal degradation, we expressed a GFP–Lamp1 fusion construct under the ubiquitous *tubulin* promoter. In *Drosophila* cells, the LAMP1-derived cytoplasmic tail is sufficient to target this fusion protein from the Golgi to late endosomes and lysosomes, where hydrolases degrade GFP (Figure 6A; Rohrer *et al*, 1996, Pulipparacharuvil *et al*, 2005). Loss of VhaPRR caused a severe accumulation of LAMP1, as opposed to the neighbouring wild-type tissue where GFP-Lamp1 was hardly detectable (Figure 6E). The accumulation was detected in both apical Lysotracker-negative and basal Lysotracker-positive compartments (Figure 6F and G). These findings suggest that apical vesicles are present, but they are less acidic in *VhaPRR* mutant cells. Moreover, these organelles seem to be unable to sort transmembrane proteins such as LAMP1 into the lysosomal degradation pathway.

Lack of VhaPRR leads to mistrafficking of E-Cadherin and cell packing defects

To test for other transmembrane proteins we immunostained for Notch and E-Cadherin. We found a strong accumulation of the intracellular domain of Notch (NICD) inside the clones (described below and in Figure 8). For E-Cadherin we detected an accumulation in intracellular vesicles, but also at the cell–cell junctions (Figure 7A–D). Immunostaining of extracellular E-Cadherin showed that the increase of junctional E-Cadherin was indeed the result of increased surface E-Cadherin and not by E-Cadherin-containing intracellular vesicles close to the surface (Figure 7B). We also found elevated levels of Armadillo, implying that adherens junction components are collectively stabilized in $VhaPRR^{\Delta 1}$ cells (Figure 7C). The stabilization was more pronounced beyond 32 h APF. At these later stages, severe defects in hexagonal cell packing became apparent inside the clones, which could be linked with the misregulation of junctional E-Cadherin (Classen *et al*, 2005).

The elevated surface levels indicated that, beyond the accumulation in the degradative pathway, the endocytic uptake of E-Cadherin may be disturbed in *VhaPRR* clones. We, therefore, performed a similar antibody uptake experiments as described above for Fmi. At the prepupal stage, E-Cadherin already showed a junctional increase, albeit to a weaker extent than at later stages (Figure 7D). Upon antibody binding and chasing at 29°C, we observed a significant internalization of the E-Cadherin/antibody complex in *VhaPRR* clones (Figure 7E). E-Cadherin accumulated in basal vesicles, and this localization pattern was significantly less commonly observed in neighbouring wild-type cells (Figure 7E). Moreover, *x–z* confocal sections demonstrated more junctional and intracellular E-Cadherin in *VhaPRR* mutant cells (Figure 7F). Taken together, our results show that the increase of surface E-Cadherin is not caused by reduced endocytic uptake but possibly via enhanced recycling.

As E-Cadherin has been shown to traffic via the Rab11-dependent recycling pathway in *Drosophila* epithelial cells (Langevin *et al*, 2005), we co-expressed *VhaPRR* RNAi and a dominant-negative form of Rab11, Rab11SN. Rab11SN, indeed, prevented the increase of junctional E-Cadherin in *VhaPRR* knockdown cells (Supplementary Figure S5B). Moreover, in our immunostainings for Rab5 and Rab11, which are early and recycling Rab GTPases, respectively, we found only a slight accumulation for Rab5 in *VhaPRR* mutant clones, but a very strong increase of Rab11 in apical sections (Supplementary Figure S6Aand B). In more basal sections, we also detected an accumulation of Rab7, most likely as a

Figure 3 PCP core proteins control VhaPRR stability. (**A**, **A′**) *Flp*-out clones expressing *Fmi* RNAi show loss of VhaPRR, also at the clone boundaries (white arrow in (**A**)). Clone area is marked by GFP and labelled with 'RNAi'. Neighbouring wild-type tissue is marked with 'wt'. (**B**, **C**) *fz* mutant clones (**B′**; marked by loss of β-gal) and *Stbm* RNAi *flp*-out (**C′**; marked by GFP) show reduction of VhaPRR. Note that VhaPRR is still present at clone boundaries (arrowheads in (**B**, **C**)). (**D**) *Flp*-out clones overexpressing Fmi (marked by GFP and 'GOF' for gain-of-function) show strong stabilization of endogenous VhaPRR at the plasma membrane. Fmi, VhaPRR (not shown) and the endosomal marker Hrs co-localize in subapical vesicles (inset in (**D′**) is a more basal confocal plane compared with (**D**, **D′**)). (**E**, **F**) By contrast, VhaPRR is strongly reduced upon Fz overexpression (**E**, **E′**; in GFP-marked *flp*-out clones) and less asymmetric upon Stbm overexpression (**F**, **F′**). Note that VhaPRR responds to the non-autonomous effects of Fz overexpression, displaying enrichment at clone boundaries (arrowhead in (**E**)) and reoriented PCP domains surrounding the clone. (**G**, **G′**, **G″**) Overexpression of myc–Fz with *ptc*-GAL4 reduces Fmi and VhaPRR at junctions. Both proteins redistribute to small intracellular vesicles. At the posterior *ptc* expression domain boundary, Fmi and VhaPRR are enriched (arrowhead in (**G″**)). (**H**) The co-overexpression of Fmi (in red; **H′**) and myc–Fz (in blue; **H″**) causes stabilization of VhaPRR (in green; **H**). All three proteins co-localize at broadened apical junctions (inset in **H″**).

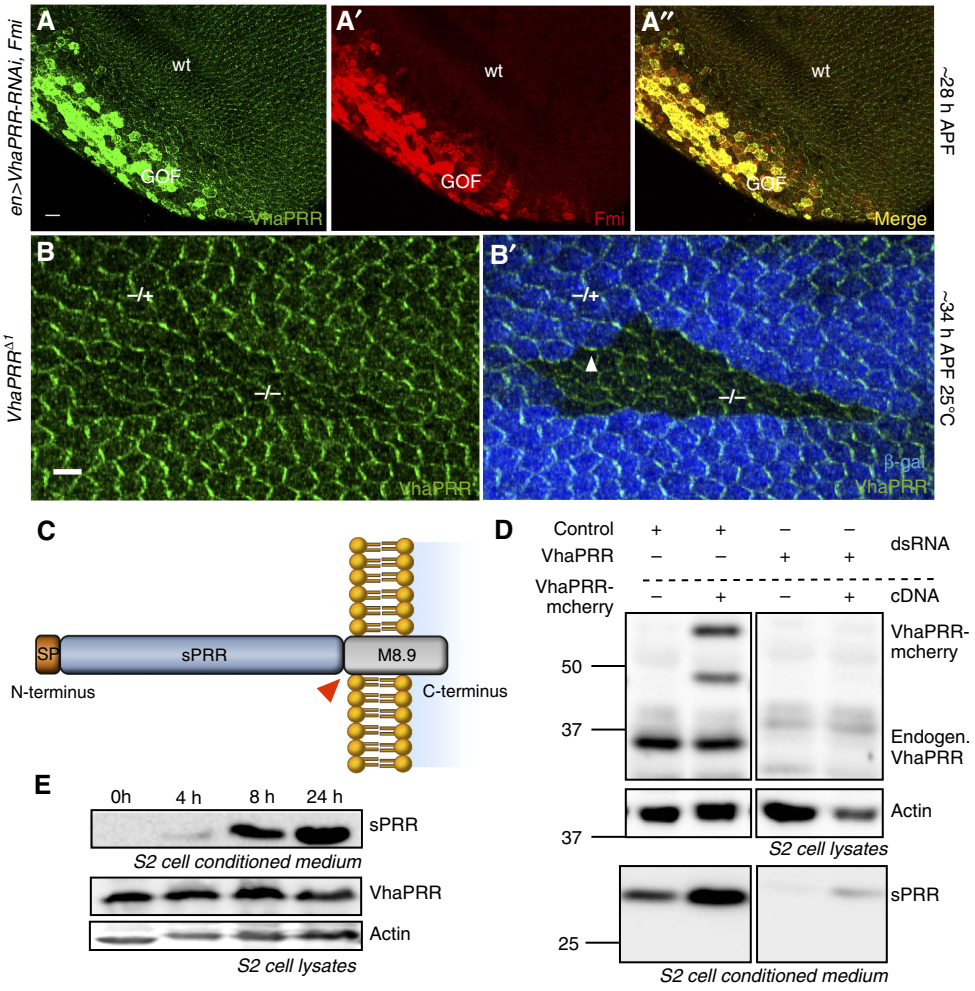

Figure 4 The extracellular part of VhaPRR, sPRR, is cleaved and secreted. (**A**, **A′**, **A″**) Co-overexpression of Fmi and *VhaPRR* RNAi (with *en*-GAL4) causes stabilization of VhaPRR (green) and co-localization with Fmi (red) in spite of RNAi expression in the posterior compartment. The reduced posterior compartment is a result of *VhaPRR* silencing. (**B**) VhaPRR reappears within the clones and at clone boundaries beyond 34 h APF. Note that also anterior–posterior (A–P) clone boundaries (arrowhead in (**B′**)) contain VhaPRR, suggesting that new PCP domains are formed here due to different levels of Fz signalling (scale bar 5 μm). (**C**) Schematic diagram of the domain structure of VhaPRR, demonstrating the extracellular domain (sPRR) and the transmembrane stump M8.9. The cleavage site (RxxR) is highlighted with a red triangle. (**D**) S2 cells were transfected with pAc-VhaPRR-mCherry or empty pAc vector, and after 48 h cells were subjected to serum starvation for 24 h for conditioned medium collection. Immunoblots of cell lysates and of the conditioned medium are shown. The extracellular part of VhaPRR (sPRR) in the conditioned medium is enhanced upon VhaPRR-mCherry overexpression. The specificity for full-length VhaPRR (upper panel) and sPRR (lower panel) bands was demonstrated by the knockdown of VhaPRR (right). VhaPRR-mCherry generates two bands with higher molecular weight than endogenous VhaPRR. Actin was used as a loading control of the lysates. (**E**) Western blot showing the time course of sPRR secretion by S2 cells. Conditioned medium was collected after 0, 4, 8 and 24 h. Cell lysates (two lower panels) show corresponding VhaPRR levels and actin as a loading control. Source data for this figure is available on the online supplementary information page.

result of the block in the endolysosomal pathway (Supplementary Figure S6C). The Golgi marker GM130 was not affected by lack of VhaPRR (Supplementary Figure S6D). Together, these results suggest that in *VhaPRR* mutant cells, E-Cadherin fails to undergo lysosomal degradation and recycles back to the surface, where it may contribute to altered hexagonal packing.

Comparison with the V-ATPase and PCP proteins

So far, our findings propose that, in addition to its PCP involvement, VhaPRR plays an important role in endocytic sorting of cargo to lysosomes. To compare both the PCP and the trafficking functions of VhaPRR with other PCP proteins and V-ATPase subunits, we used several genetic approaches to disrupt PCP signalling and V-ATPase function. The following parameters were compared (Figure 8; Supplementary Figure S7): wing hair polarity, Fz localization, co-localization with PCP domains, organellar acidification, endolysosomal degradation and junctional E-Cadherin levels.

Our efforts to genetically manipulate V-ATPase subunits by RNAi or mutant alleles resulted in no phenotypes or strong cell-toxic effects and elimination of clones (Supplementary Figure S4B–D and not shown). Best survival of clones was achieved with a *Vha68-2* allele (Vaccari *et al*, 2010), but the survival period was shorter compared with *VhaPRR* clones. In these clones, PCP was mostly unaffected (Figure 8C and F). In some clones, there was a delay in wing hair formation and some Fz mislocalization (not shown). However, these phenotypes were much weaker than in *VhaPRR* or *Fmi* RNAi clones and may be secondary to the reduced viability

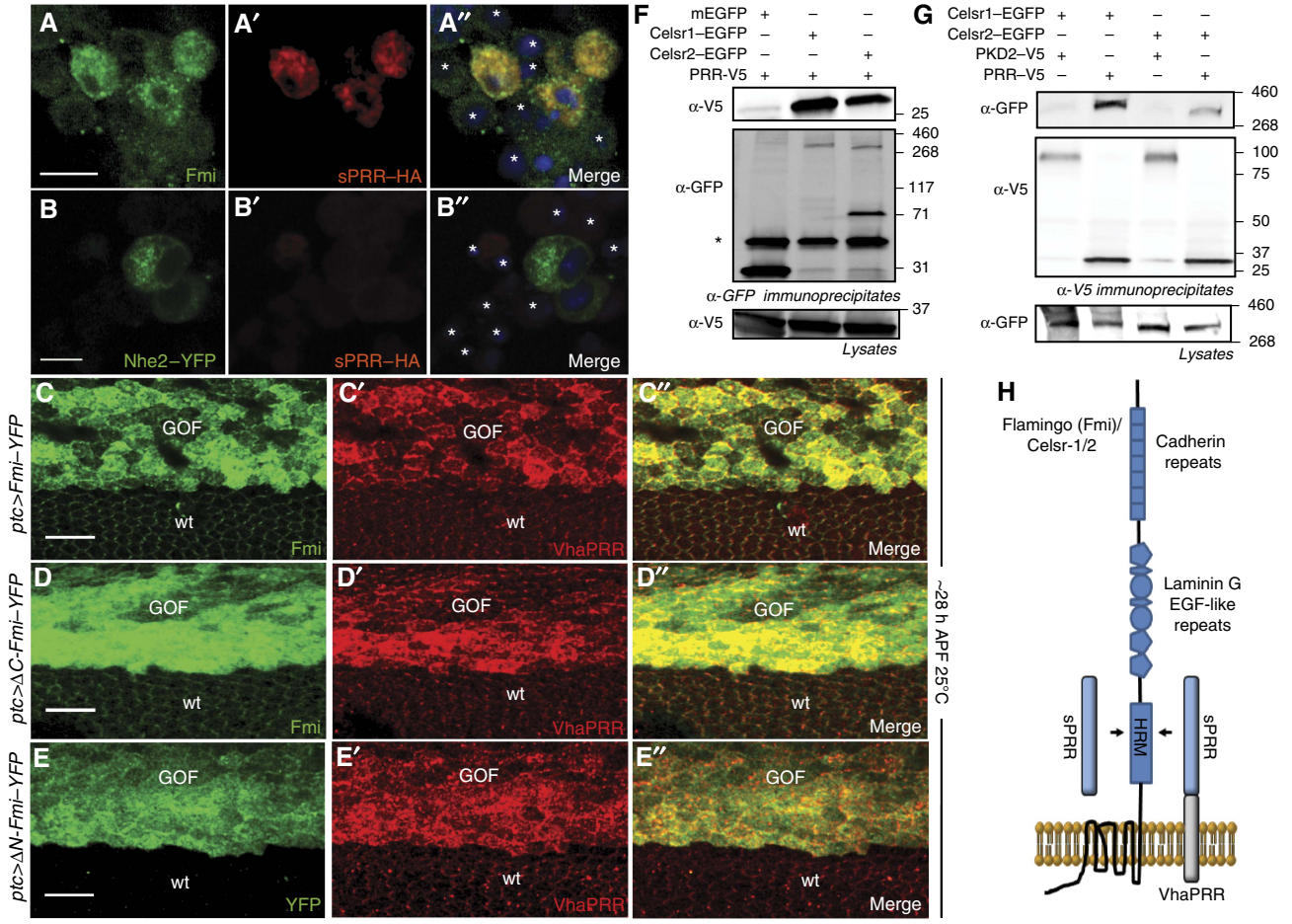

Figure 5 VhaPRR and Fmi physically interact. (**A**, **B**) Conditioned medium containing sPRR–HA was applied to S2 cells transfected with Fmi (**A**) or a control protein Nhe2–YFP (**B**). (**A**–**A**″) sPRR–HA (red), detected by immunostaining with an anti-HA antibody, predominantly bound to Fmi-positive cells (green) and not to untransfected cells (asterisks) or Nhe2 expressing cells (**B**′, **B**″). The non-transfected cells in (**A**) show a weak signal with anti-Fmi due to endogenous Fmi. (**C**–**C**″) Overexpression of Fmi–YFP with *ptc*-GAL4 causes stabilization of endogenous VhaPRR. (**D**, **E**) This effect is mimicked by using a Fmi construct that lacks the intracellular part (ΔC-Fmi; **D**–**D**″) and by Fmi that lacks most of the extracellular part (ΔN-Fmi; **E**–**E**″). The small so-called HRM-domain and the extracellular transmembrane loops are the only overlapping parts of Fmi between these constructs.(**F**) V5-tagged PRR (PRR–V5; from *X. laevis*) was co-expressed with Celsr-1- or Celsr-2–EGFP (from mouse) and a control transmembrane protein (PKD2–V5) in HEK293T cells. After immunoprecipitation with anti-GFP, PRR–V5 bound to immunoprecipitated Celsr-1 and Celsr-2, but not to the control protein mEGFP. The asterisk marks the heavy chain bands of the GFP antibody. (**G**) In a similar fashion, Celsr-1 and Celsr-2 were present in immunoprecipitates formed by PRR–V5, but not by the control transmembrane protein PKD2–V5. (**H**) A schematic diagram shows the interaction (arrows) between the extracellular domain of VhaPRR or sPRR with the HRM and/or the extracellular loops of the heptahelical protocadherin Fmi (or Celsr-1/2). Note that the sizes of the boxes and shapes do not represent the actual sizes of the respective domains. Source data for this figure is available on the online supplementary information page.

(Figure 8A–E). To test for a PCP-like localization pattern of V-ATPase subunits, we used GFP trap lines for Vha55 and Vha16 (not shown) as well as an antibody against Vha44. Specificity of the antibody and the proper insertion of the GFP gene trap into the endogenous *Vha55* locus was confirmed by RNAi-mediated silencing of Vha44 and Vha55, respectively (Figure 8F; Supplementary Figure S4B). These subunits showed a diffuse punctate pattern and no enrichment at the asymmetric PCP domains. Moreover, overexpression of Fmi stabilized VhaPRR but not Vha55–GFP (Supplementary Figure S4E).

To compare endosomal trafficking effects, we used Lysotracker as well as GFP–LAMP1, E-Cadherin and Notch receptor localization. Consistent with previous results (Yan *et al*, 2009; Vaccari *et al*, 2010), *Vha68-2* mutant clones showed a reduced number of Lysotracker-positive compartments (Figure 8L). Unlike VhaPRR clones, there was also reduction in basal Lysotracker uptake (inset in Figure 8L). Endolysosomal degradation defects were demonstrated by increased Notch and GFP–LAMP1 in *Vha68-2* mutant clones and in *Vha26* knockdown cells, respectively (Figure 8O; Supplementary Figure S7I). Junctional E-Cadherin was enhanced in *Vha68-2* clones but to a smaller extent than in *VhaPRR* clones (Figure 8Q and R). Likewise, Vha68-2 removal caused weaker apical Rab11 accumulation than VhaPRR removal (Supplementary Figure S7A), suggesting that VhaPRR has a more specific role in apical recycling.

By contrast, lack of PCP core proteins did not seem to affect membrane trafficking. We could not detect any changes in Lysotracker uptake, Notch, E-Cadherin and LAMP1 localization in *Fmi* RNAi and fz^{P21} clones (Figure 8J, M and P; Supplementary Figure S7D–G). Taken together, these results suggest that Fmi and Fz do not share the endosomal trafficking function with VhaPRR. By contrast, the V-ATPase shows

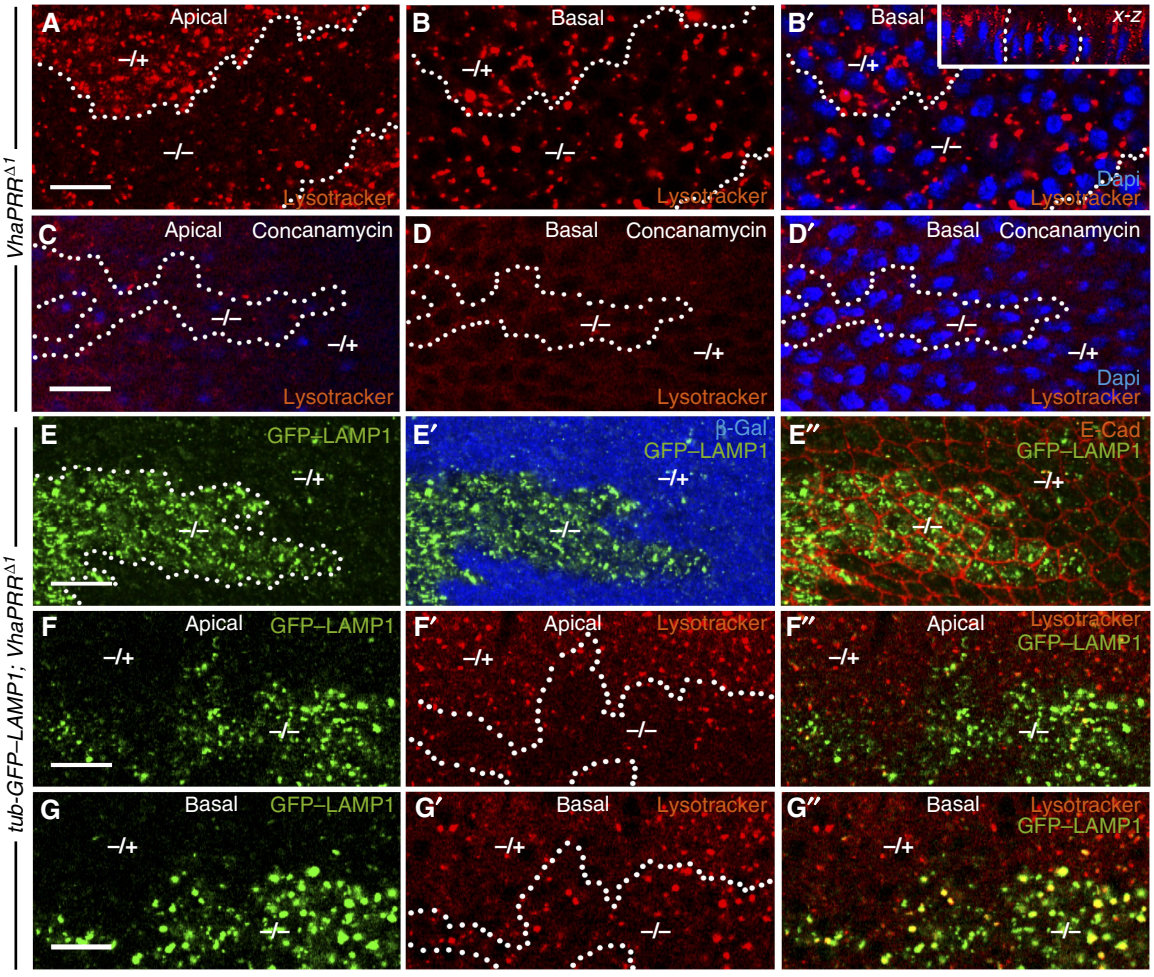

Figure 6 VhaPRR regulates vesicular acidification and lysosomal degradation. (**A**, **B**) Prepupal wings (5 h APF) were incubated with Lysotracker (red). In apical sections of *VhaPRR* clones (within dotted line), vesicular Lysotracker uptake was reduced compared with the wild-type tissue (**A**). In more basal sections, overall uptake was comparable, although some Lysotracker-positive vesicles within the clones appeared enlarged (**B**, **B**′). Nuclei (in blue) are normal in number and appearance inside the clone (**B**′). A *x*–*z* projection of another clone is presented in the inset of (**B**′). Here, apical is up and basal is down. Note the absence of apical Lysotracker signal. (**C**, **D**) Pretreatment with the V-ATPase inhibitor Concanamycin A abolished most of the Lysotracker signal in apical (**C**) and basal (**D**, **D**′) sections of wild-type and mutant cells. (**E**, **E**′) The ubiquitously expressed GFP–LAMP1 strongly accumulates in cells mutant for *VhaPRR*, suggesting impaired endolysosomal maturation in pupal wings at 28 h APF. E-Cadherin staining in (**E**″) shows cell outlines. (**F**, **F**′, **F**″, **G**, **G**′, **G**″) Combined Lysotracker uptake and visualization of GFP–LAMP1 shows compartments that accumulate LAMP1 but lack acidification. Most of these compartments can be found in apical cell sections (**F**′, **F**″).

overlapping functions with VhaPRR in the endosomal but not in the PCP pathway (schematic model in Figure 9).

Discussion

Previous studies have shown that the PCP transmembrane proteins are key to forming an intrinsically asymmetric complex in the pupal wing cells. Here, we make the unexpected finding that the transmembrane protein VhaPRR shares decisive characteristics with the other PCP core proteins: (1) PCP phenotypes in various fly tissues, (2) an asymmetric localization, (3) the reciprocal stabilization of PCP core proteins within PCP domains and (4) the physical interaction with other PCP core components, with Fmi as the primary binding partner.

Current models propose that polarized transport from the *trans*-Golgi network or recycling endosomes is important for the formation of PCP domains at P–D boundaries (Shimada *et al*, 2006; Strutt and Strutt, 2008; Harumoto *et al*, 2010; Strutt *et al*, 2011). The directionality is provided by different levels of Fz signalling between neighbouring cells in the P–D axis, induced by a poorly understood cue (Goodrich and Strutt, 2011). Fmi seems to be the first among the PCP proteins to sense these differences and to become recruited to the nascent PCP domains (Usui *et al*, 1999). An asymmetric Fz–Fmi:Fmi complex can be formed in the absence of Stbm, suggesting that this complex is the primary building block for the PCP domains (Chen *et al*, 2008; Strutt and Strutt, 2008; Strutt *et al*, 2011). Recent evidence also suggests that the Fz–Fmi:Fmi bridges are sufficient to polarize cells in the plane of the epithelium (Struhl *et al*, 2012). Once the complex has been formed at the proper cell boundary, it is maintained and amplified by endocytic removal. Whereas non-complexed PCP components are subject to internalization, PCP molecules associated with the asymmetric PCP domains become refractory to endocytic turnover (Strutt *et al*, 2011).

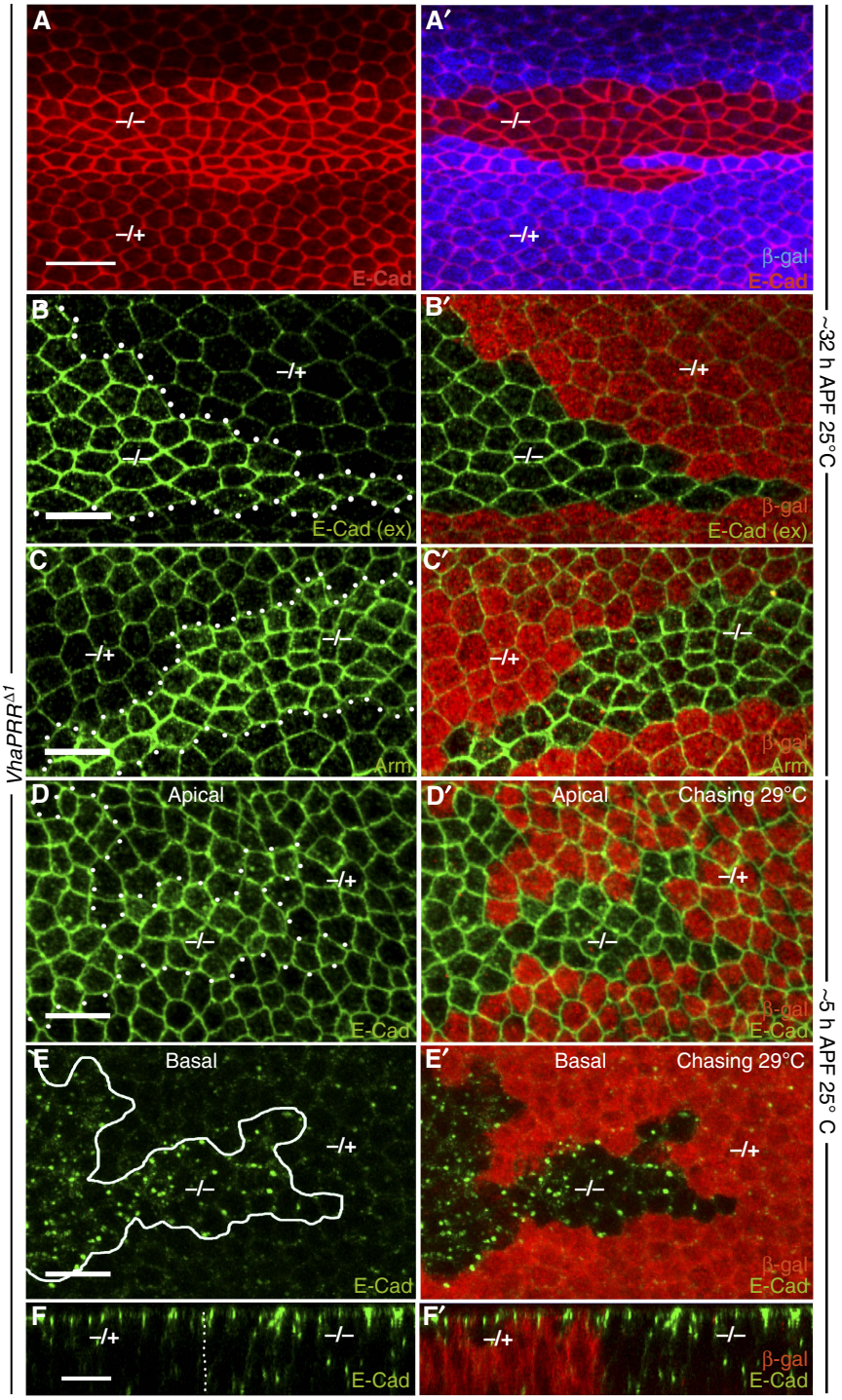

Figure 7 Lack of VhaPRR causes cell packing defects and increases junctional E-Cadherin. (**A**, **A**′) E-Cadherin (red) levels are elevated in *VhaPRR* mutant clones at 32 h APF. Lack of β-gal (blue in **A**′) marks the clone region. Hexagonal packing is strongly impaired, with less hexagons but more pentagons and heptagons compared with the hexagonal wild-type cells outside the clone. The cell size is also variable. Note that the clone lies above a vein that also shows increased E-Cadherin levels. (**B**) Extracellular E-Cadherin (green) staining (without detergent) demonstrates increased surface levels. Here (**B**′) and in the remaining panels, β-gal is shown in red. (**C**, **C**′) Armadillo (Arm; green) is also increased inside the clones. (**D**–**F**) Antibody uptake experiments in prepupal wings show that E-Cadherin is readily endocytosed upon antibody binding. (**D**, **D**′) Apical sections of a prepupal wing with a chase carried out at 29°C shows that junctional E-Cadherin is elevated inside the mutant clones. (**E**, **E**′, **F**, **F**′) In more basal sections, the same clone displays a strong accumulation of E-Cadherin in intracellular vesicles (inside white circle in (**E**)), compared with the neighbouring wild-type tissue. (**F**) A *x*–*z* projection shows the increase of E-Cadherin both at adherens junctions and in intracellular vesicles in mutant clones. E-Cadherin-positive basal vesicles are rarely seen in wild-type cells.

VhaPRR and its truncated version sPRR precisely follow the Fmi localization pattern during PCP domain formation. Although both Fmi and Fz are able to bind VhaPRR (this work and Buechling *et al*, 2010; Hermle *et al*, 2010), only Fmi seems to be able to stabilize VhaPRR. This difference is particularly obvious when Fmi and Fz are overexpressed

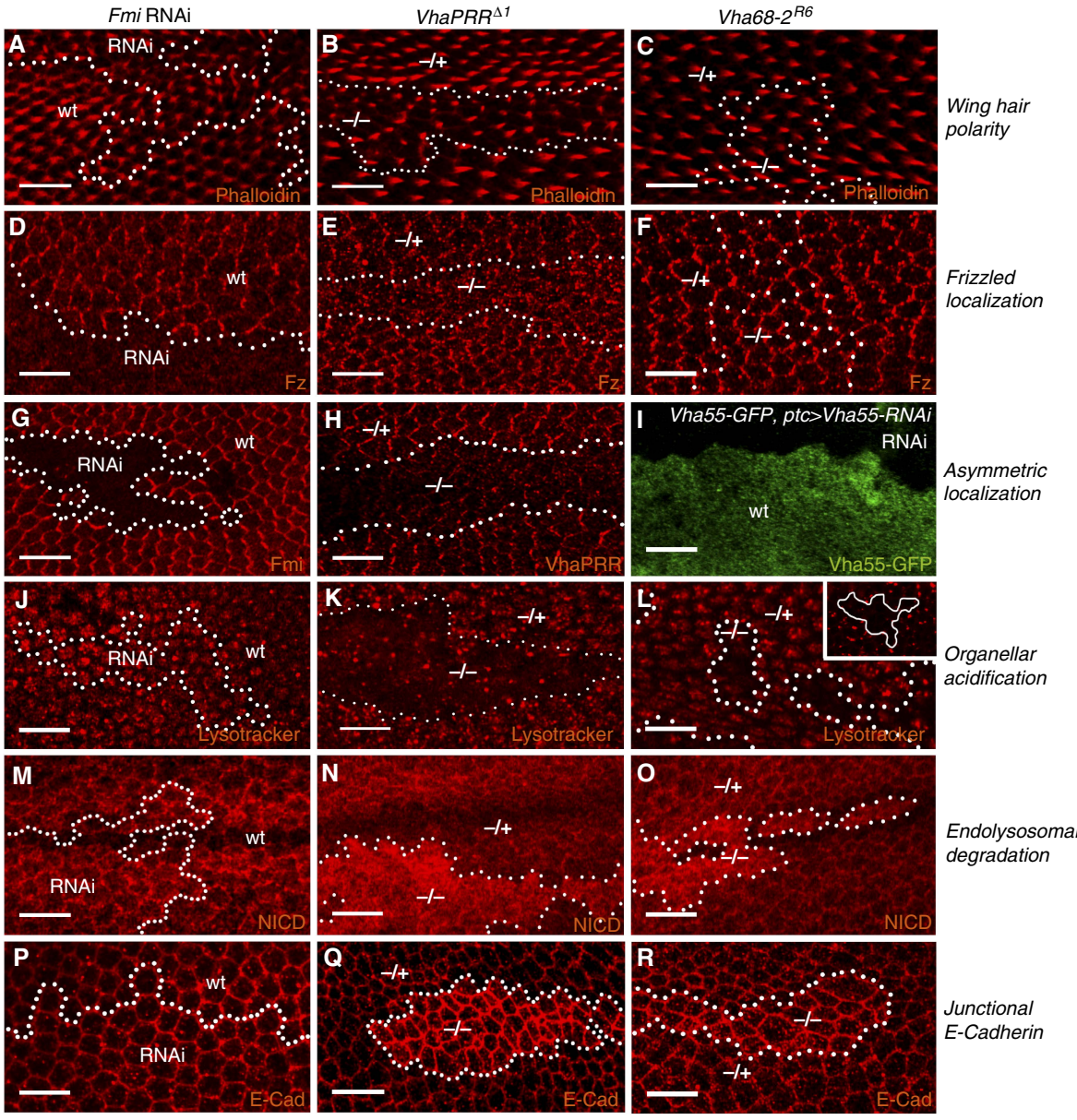

Figure 8 Comparison of PCP and membrane trafficking defects. *Fmi* RNAi, *VhaPRR* and *Vha68-2* clones (28 h APF unless otherwise stated) are compared with respect to: (**A**–**C**) Wing hair polarity: Hairs are stained with Rhodamine-phalloidin at 32–33 h APF; (**D**–**F**) Fz localization; (**G**–**I**) Asymmetric localization: *Fmi* RNAi (**G**) and *VhaPRR* (**H**) clones show loss of protein inside the clone. Outside the clone, the asymmetric distribution is evident. (**I**) To assess V-ATPase subunit localization Vha55–GFP is used, which is an insertion of GFP in the genomic locus; Vha55–GFP does not show an asymmetric PCP-like distribution. The GFP signal is completely removed by *ptc*-GAL4-mediated co-expression of Vha55-RNAi (upper part), demonstrating the validity of this GFP trap line; (**J**–**L**) Acidification: **J**–**L** are apical sections, and inset in **L** is a basal section; (**M**–**O**) Notch localization; (**P**–**R**) E-Cadherin localization in apical sections to demonstrate junctional levels; See text for more explanation, and Supplementary Figure 7 for more genotypes.

(Figure 3D, E, G and H). Our data suggest that, once recruited to PCP domains by Fmi, VhaPRR/sPRR contribute to complex stabilization, possibly by functioning as an adaptor between Fz and Fmi. Lack of VhaPRR leads to increased internalization of PCP proteins and, eventually, to PCP phenotypes, such as wing hair mispolarization. Unlike other transmembrane proteins described in this study, PCP proteins do not appear to accumulate in the endolysosomal pathway. Where they turn out to be is currently unclear, as we were unable to detect significant co-localization of PCP proteins with organellar markers in *VhaPRR* clones (not shown).

An interesting finding is that ectopic VhaPRR and sPRR are unable to localize to PCP domains (Supplementary Figure S3B and C). This suggests that the exogenous proteins lack a necessary modification, or that the binding sites are saturated by the endogenous protein. It is therefore conceivable that incorporation of VhaPRR into the PCP domains requires a precise stochiometry, only accessible for a limited pool of VhaPRR. Upon incorporation, VhaPRR itself contributes to the 'locked-in' state of the low-turnover PCP domains.

Does VhaPRR participate in V-ATPase-related functions? By using Lysotracker, we could show that in *VhaPRR* mutant clones apical vesicles seemed less acidic. This effect was slightly different than in *Vha68-2* clones. Removal of this subunit led to a more general impairment of organellar acidification, which may be a reason for the stronger impact

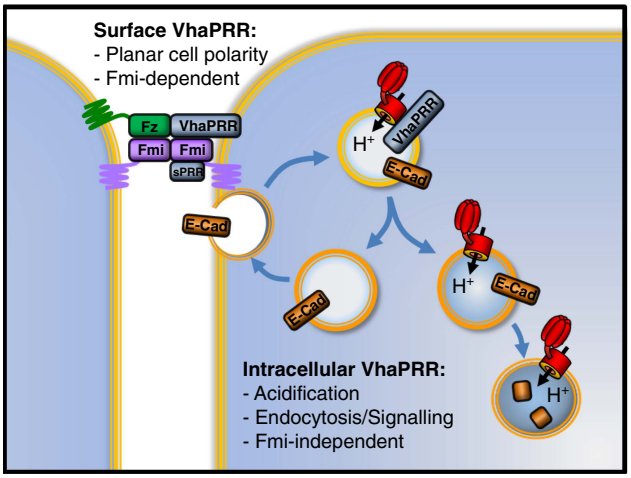

Figure 9 Model of the proposed dual functions of VhaPRR. Surface VhaPRR functions in PCP. Both sPRR and full-length VhaPRR can be recruited to the PCP domains by Fmi. Intracellular VhaPRR contributes to the acidification of apical endosomes in conjunction with the H^+-pumping V-ATPase (in red). It also promotes sorting of cargo for degradation in lysosomes (lower right). These functions seem to be Fmi-independent. In the absence of VhaPRR, E-Cadherin (E-Cad) recycles more readily to the cell surface and endosomal signalling (e.g., Notch and canonical Wnt signalling) is impaired. Please note that different protein drawings do not reflect the actual sizes of the proteins.

on cell viability. The disturbances in the degradative pathway were comparable between *VhaPRR* and *Vha68-2* mutant cells and *Vha26* knockdown cells, respectively. Defective degradation was observed for E-Cadherin, Notch and LAMP1. Moreover, Notch accumulation along with compromised Notch signalling was previously observed in *Vha68-2*, *Vha55* and *VhaAC39* mutant cells (Yan *et al*, 2009; Vaccari *et al*, 2010). Therefore, the degradation defect is most likely a result of altered V-ATPase activity and, possibly, of impaired directionality in endolysosomal maturation (Storrie and Desjardins, 1996; Williamson *et al*, 2010). A reduction of vesicular acidification by loss of VhaPRR is also consistent with the reported involvement of ATP6AP2/PRR and the V-ATPase in the canonical Wnt signalling pathway (Buechling *et al*, 2010; Cruciat *et al*, 2010; Hermle *et al*, 2010). An important activation step in this pathway is the phosphorylation of the Wnt co-receptor LRP6 in acidic endosomes (Cruciat *et al*, 2010). Therefore, it would be interesting to see how the canonical Wnt receptor Fz2 and LRP6/Arrow are affected by removal of VhaPRR. In any case, the results shown here support a shared role of VhaPRR and the V-ATPase in the endolysosomal pathway and its associated signalling events.

Within the PCP pathway, there is, on the other hand, less overlap between VhaPRR and the V-ATPase. In most *Vha68-2* mutant clones, there were no PCP defects. Importantly, we failed to detect any PCP-like localization patterns or Fmi-induced stabilization for V-ATPase subunits other than VhaPRR. Nevertheless, it cannot be ruled out that a specific V-ATPase subpool functions in PCP, for example, in the transport of PCP proteins to PCP domains. Therefore, more tools are needed for genetic manipulation and visualization of other subunits as well as for more compartment-specific pH measurements.

If the V-ATPase does not function in PCP, but performs overlapping functions with VhaPRR in endosomal trafficking, an important remaining question is whether the core PCP proteins can also control membrane trafficking (Classen *et al*, 2005; Mottola *et al*, 2010). We could not find any defects in vesicular acidification and Notch trafficking in Fmi RNAi and fz^{P21} clones. Also, E-Cadherin localization was largely normal compared with *VhaPRR* or *Vha68-2* clones. It can therefore be concluded that lack of Fz and Fmi strongly affects the junctional pool of VhaPRR, but most likely not the membrane trafficking or vesicular pool.

In summary, our data point towards a dual function for VhaPRR: one as a novel PCP core protein and the other as a regulator of endosomal trafficking (see model in Figure 9). Studying VhaPRR could lead to further valuable insights for the general understanding of PCP domain establishment and of endocytic sorting mechanisms. Important open questions are, for example, how the two functions of VhaPRR are regulated and whether crosstalk between them can potentially come into play. As the endosomal function seems to be linked with the V-ATPase, it is intriguing to speculate that the acidic pH in endosomes induces conformational changes and/or post-translational modifications of VhaPRR that are not present in the surface pool. Vice versa, PCP-specific alterations of the protein might be facilitated by neutral pH and/or prevented by acidic pH. Given that mutations in ATP6AP2/PRR cause mental retardation and epilepsy in humans (Ramser *et al*, 2005), it will also be important to see what functions of this protein are crucial for other cell types, such as neurons. Thus, our functional characterization in *Drosophila* has introduced novel features of VhaPRR that may have important implications for diverse developmental and disease contexts.

Materials and methods

Fly strains and genetics

Overexpression and transgenic RNAi studies were performed using the UAS/GAL4 system (RNAi crosses grown at 25 or 29°C). *VhaPRR* RNAi lines were described previously (Hermle *et al*, 2010). $VhaPRR^{\Delta 1}$ harbours an 860-bp-deletion in the *VhaPRR* locus and was created by imprecise excision of the P-element EY03616 from the Bloomington Stock Centre (line 15665) using the Δ2–3 transposase. Excision of the P element was confirmed by polymerase chain reaction and sequencing. The allele was recombined onto a neoFRT82b chromosome for mosaic analysis. Clones were made with *hs-flp or ubx-flp. ptc*-GAL4 (from N Perrimon) and *en*-GAL4 (from the Bloomington; also contains UAS-Dicer2 and UAS–GFP) were used for wing expression. Heat shock-induced *flp*-out clones were under the control of the *act*-GAL4. $Vha68\text{-}2^{R16}$, fz^{P21}, UAS-Fz, UAS-Stbm and UAS-fmi strains were as described previously (Jenny *et al*, 2003; Wu *et al*, 2004; Hermle *et al*, 2010; Vaccari *et al*, 2010). Other lines included *tubulin(tub)*-GFP–LAMP1 (by H Krämer). Vha44 (ID:101527), Vha26 (ID:102378), Fmi (ID:107993) and Stbm (ID:100819) RNAi lines were from the Vienna *Drosophila* RNAi centre (VDRC). The Vha55–GFP gene trap line (ID:115558) is from the Kyoto stock centre. To generate VhaPRR-expressing transgenic flies, we cloned sPRR–HA, VhaPRR and VhaPRR (AxxA) into pUASg-attB (from K Basler) and injected it into flies with an attP landing site at 86FB by Bestgene. The rescue construct harboured the full 2.6 kb-genomic locus of *VhaPRR*. Primer sequences and cloning details are available in the Supplementary Data.

Immunostaining and live imaging

Pupal wings were dissected, fixed in 8% paraformaldehyde for 45 min (wings) or 4% paraformaldehyde for 20 min (other tissues), and stained according to the standard procedure. The following

primary antibodies were used: guinea pig anti-Hrs (1:500, by HJ Bellen), rabbit anti-Rab5 (1:5000), rabbit anti-Rab7 (1:3000), rabbit anti-Rab11 (1:5000; all by A Nakamura), mouse anti-Rab11 (1:100; BD Transduction), rabbit anti-Fz (1:200, by D Strutt), rabbit anti-Stbm (1:200, by D Strutt), rabbit anti-β-galactosidase (1:1000; MP Biomedicals), rabbit anti-GFP (1:500; MBL), mouse anti-GFP (1:50; Santa Cruz), rabbit anti-HA (1:200; Roche), mouse anti-NICD (1:50), mouse anti-Fmi (1:50), rat anti-E-cadherin (1:40), mouse anti-β-galactosidase (1:40; all by DSHB), rabbit anti-GM130 (1:1000; Abcam). The following sequence of VhaPRR was used to generate a polyclonal antibody in guinea pigs: NRPKAISFKGNDALE. For F-actin and nuclei visualization, Rhodamine-Phalloidin (1:1000; from Invitrogen) and HOE33342 (1:1000; from Invitrogen) were used, respectively.

To measure intravesicular acidification, prepupal wings were dissected, incubated for 5 min at RT with LysoTracker red DND99 (0.2 μM; Invitrogen) in PBS and immediately analysed. V-ATPase activity was blocked with Concanamycin A1 (150 nM; Sigma) treatment for 10 min at RT in PBS.

Antibody uptake experiments were performed as previously described (Strutt *et al*, 2011). Briefly, prepupa were dissected 5 h APF in Schneider's medium containing 10% FCS. The wings were incubated with primary antibodies (mouse anti-Fmi #71 (kind gift of D Strutt) and rat anti-E-Cadherin (DSHB); dilution 1:10 each) for 30 min at 4°C and chased at 29 or 4°C, respectively, for 45 min. Endocytosis was stopped by transferring the wings in fresh Schneider's medium with FCS at 4°C for 5 min. The tissue was then fixed and stained and analysed with confocal microscopy according to the standard immunostaining protocol.

For imaging, a Zeiss LSM 510 confocal microscope was used, and for image processing ImageJ and Adobe Photoshop CS4 software. Quantification of Fmi uptake was performed with Image J software. A maximum of three confocal sections with the highest staining intensity for Fmi were averaged and a default threshold was applied. Then, the average fluorescence of mutant regions was set in a ratio to the surrounding wild-type regions. In total, at least five experiments (including one or two wings each) were scored for the permissive and the non-permissive temperature. Error bars represent standard error of the mean, and statistical significance was determined using unpaired Student's *t*-test ($P<0.01$).

S2 cell experiments

S2 cells were propagated in Schneider's medium (BIOTECH) supplemented with 10% FCS (Sigma). For the Fmi-binding assay, cells were transfected with pRmHA3-Fmi, using Effectene (Qiagen). Expression of full-length Fmi was induced by the addition of 0.7 mM $CuSO_4$ 18 h after transfection. The medium was replaced 24 h later with conditioned medium from sPRR–HA-expressing cells or untransfected cells. After 1 h of incubation at room temperature, we fixed and immunostained cells (with mouse anti-Fmi (1:50, DSHB) and rat anti-HA (1:200, Roche) according to the standard procedure.

For western blot, 1×10^6 S2 cells/well were transfected with the following cDNA constructs: empty pAc, pAc-VhaPRR-mcherry and pUAST-VhaPRR–HA or pUAST-VhaPRR RxxR (both co-transfected with pAc-GAL4). After 42 h of incubation at 25°C, cells were serum-starved for 24 h. Conditioned medium was centrifuged at 3000 r.p.m., and the supernatant was concentrated using Amicon Ultra-4 filters (Millipore). Cells were resuspended in 1 ml of D-PBS and centrifuged for 5 min at 3000 r.p.m. The pellet was resuspended in 100 μl of ice-cold Lysis Buffer containing 50 mM TRIS pH 7.4, 150 mM NaCl, 50 mM NaF, 1 mM EDTA, 1% Triton X-100, protease inhibitors (Roche), and 1,5 mM Na_3VO_4. The lysate was incubated in ice for 30 min and then centrifuged at 13 000 r.p.m. for 15 min. In all, 6 × Laemmli buffer was added to the samples before loading them on a 15% SDS–polyacrylamide gel. Proteins were transferred to a PVDF membrane (Millipore). VhaPRR was detected by western blotting using a guinea pig polyclonal anti-VhaPRR. For loading control, a mouse monoclonal anti-β-actin (Sigma) was used.

Knockdown of VhaPRR in S2 cells was performed as explained in the DRSC website (http://www.flyrnai.org). In total, 5 μg dsRNA targeted against VhaPRR was used for 7.5×10^5 of S2 cells. Cells were incubated for 4 days before analysis.

Co-immunoprecipitation experiments

Co-immunoprecipitations were performed as described previously (Simons *et al*, 2005). Briefly, HEK293T cells were transiently transfected using FuGENE HD Transfection Reagent (Roche) with PRR–V5 (kind gift by C Niehrs) and Celsr-1–EGFP or Celsr-2–EGFP (kind gift by E Fuchs) and the control proteins PKD2–V5 and mEGFP, respectively. After incubation for 24 h, cells were washed and lysed in a buffer containing 20 mM Tris–HCl (pH 7.5), 1% Triton X-100, 50 mM NaF, 15 mM Na_4P2O_7, 0.1 mM EDTA, 150 mM NaCl, 1 mM Na_3VO_4, and protease inhibitors and incubated in ice for 30 min. After centrifugation (13 000 r.p.m., 60 min, 4°C), cell lysates containing equal amounts of total protein were incubated for 1.5 h at 4°C with antibody-bound protein G Sepharose beads (GE Healthcare) for 1.5 h. The beads were washed extensively with lysis buffer, and bound proteins were resolved by SDS–PAGE. The following antibodies were used: mouse anti-GFP (1:500, Santa Cruz), rabbit anti-GFP (1:1000, MBL) and mouse anti-V5 (1:500, Serotec).

Supplementary data

Supplementary data are available at *The EMBO Journal* Online (http://www.embojournal.org).

Acknowledgements

We thank Giorgos Pyrowolakis, Marek Mlodzik, David Strutt, Hugo Bellen, Tadashi Uemura, Suzanne Eaton, Thomas Vaccari, Helmut Krämer, Norbert Perrimon, the Bloomington and Kyoto Stock Centers as well as the VDRC for fly strains. We thank Christof Niehrs, Michael Boutros, Elaine Fuchs and Konrad Basler for cDNA constructs. We thank the DSHB for antibodies, as well as Julian Dow, David Strutt, Hugo Bellen and Akira Nakamura. We acknowledge Roland Nitschke from the Life Imaging Center Freiburg for help with confocal microscopy. We thank Giorgos Pyrowolakis, Marek Mlodzik, Annette Schenck and Jochen Rink for critically reading the manuscript. The work has been supported by an Emmy-Noether Grant SI1303/2-1 by the Deutsche Forschungsgemeinschaft.

Author contributions: TH, MCG and MS designed the experiments. TH, MCG, SB and SH performed the experiments. MS wrote the paper.

Conflict of interest

The authors declare that they have no conflict of interest.

References

Aigouy B, Farhadifar R, Staple DB, Sagner A, Roper JC, Julicher F, Eaton S (2010) Cell flow reorients the axis of planar polarity in the wing epithelium of *Drosophila*. *Cell* **142:** 773–786

Axelrod JD (2001) Unipolar membrane association of Dishevelled mediates Frizzled planar cell polarity signaling. *Genes Dev* **15:** 1182–1187

Bastock R, Strutt H, Strutt D (2003) Strabismus is asymmetrically localised and binds to Prickle and Dishevelled during *Drosophila* planar polarity patterning. *Development* **130:** 3007–3014

Bayly R, Axelrod JD (2011) Pointing in the right direction: new developments in the field of planar cell polarity. *Nat Rev Genet* **12:** 385–391

Buechling T, Bartscherer K, Ohkawara B, Chaudhary V, Spirohn K, Niehrs C, Boutros M (2010) Wnt/Frizzled signaling requires dPRR, the *Drosophila* homolog of the prorenin receptor. *Curr Biol* **20:** 1263–1268

Chen WS, Antic D, Matis M, Logan CY, Povelones M, Anderson GA, Nusse R, Axelrod JD (2008) Asymmetric homotypic interactions

of the atypical cadherin flamingo mediate intercellular polarity signaling. *Cell* **133:** 1093–1105

Classen AK, Anderson KI, Marois E, Eaton S (2005) Hexagonal packing of *Drosophila* wing epithelial cells by the planar cell polarity pathway. *Dev Cell* **9:** 805–817

Cousin C, Bracquart D, Contrepas A, Corvol P, Muller L, Nguyen G (2009) Soluble form of the (pro)renin receptor generated by intracellular cleavage by furin is secreted in plasma. *Hypertension* **53:** 1077–1082

Cruciat CM, Ohkawara B, Acebron SP, Karaulanov E, Reinhard C, Ingelfinger D, Boutros M, Niehrs C (2010) Requirement of prorenin receptor and vacuolar H+-ATPase-mediated acidification for Wnt signaling. *Science* **327:** 459–463

Dietzl G, Chen D, Schnorrer F, Su KC, Barinova Y, Fellner M, Gasser B, Kinsey K, Oppel S, Scheiblauer S, Couto A, Marra V, Keleman K, Dickson BJ (2007) A genome-wide transgenic RNAi library for conditional gene inactivation in *Drosophila*. *Nature* **448:** 151–156

Forgac M (2007) Vacuolar ATPases: rotary proton pumps in physiology and pathophysiology. *Nat Rev Mol Cell Biol* **8:** 917–929

Goodrich LV, Strutt D (2011) Principles of planar polarity in animal development. *Development* **138:** 1877–1892

Gubb D, Green C, Huen D, Coulson D, Johnson G, Tree D, Collier S, Roote J (1999) The balance between isoforms of the prickle LIM domain protein is critical for planar polarity in *Drosophila* imaginal discs. *Genes Dev* **13:** 2315–2327

Harumoto T, Ito M, Shimada Y, Kobayashi TJ, Ueda HR, Lu B, Uemura T (2010) Atypical cadherins Dachsous and Fat control dynamics of noncentrosomal microtubules in planar cell polarity. *Dev Cell* **19:** 389–401

Hermle T, Saltukoglu D, Grunewald J, Walz G, Simons M (2010) Regulation of Frizzled-dependent planar polarity signaling by a V-ATPase subunit. *Curr Biol* **20:** 1269–1276

Jenny A, Darken RS, Wilson PA, Mlodzik M (2003) Prickle and Strabismus form a functional complex to generate a correct axis during planar cell polarity signaling. *Embo J* **22:** 4409–4420

Kinouchi K, Ichihara A, Sano M, Sun-Wada GH, Wada Y, Kurauchi-Mito A, Bokuda K, Narita T, Oshima Y, Sakoda M, Tamai Y, Sato H, Fukuda K, Itoh H (2010) The (Pro)renin receptor/ATP6AP2 is essential for vacuolar H+-ATPase assembly in murine cardiomyocytes. *Circ Res* **107:** 30–34

Langevin J, Morgan MJ, Sibarita JB, Aresta S, Murthy M, Schwarz T, Camonis J, Bellaiche Y (2005) *Drosophila* exocyst components Sec5, Sec6, and Sec15 regulate DE-Cadherin trafficking from recycling endosomes to the plasma membrane. *Dev Cell* **9:** 365–376

Lee H, Adler PN (2002) The function of the frizzled pathway in the *Drosophila* wing is dependent on inturned and fuzzy. *Genetics* **160:** 1535–1547

Ludwig J, Kerscher S, Brandt U, Pfeiffer K, Getlawi F, Apps DK, Schagger H (1998) Identification and characterization of a novel 9.2-kDa membrane sector-associated protein of vacuolar proton-ATPase from chromaffin granules. *J Biol Chem* **273:** 10939–10947

Mottola G, Classen AK, Gonzalez-Gaitan M, Eaton S, Zerial M (2010) A novel function for the Rab5 effector Rabenosyn-5 in planar cell polarity. *Development* **137:** 2353–2364

Nguyen G, Delarue F, Burckle C, Bouzhir L, Giller T, Sraer JD (2002) Pivotal role of the renin/prorenin receptor in angiotensin II production and cellular responses to renin. *J Clin Invest* **109:** 1417–1427

Oshima Y, Kinouchi K, Ichihara A, Sakoda M, Kurauchi-Mito A, Bokuda K, Narita T, Kurosawa H, Sun-Wada GH, Wada Y, Yamada T, Takemoto M, Saleem MA, Quaggin SE, Itoh H (2011) Prorenin receptor is essential for normal podocyte structure and function. *J Am Soc Nephrol* **22:** 2203–2212

Pulipparacharuvil S, Akbar MA, Ray S, Sevrioukov EA, Haberman AS, Rohrer J, Kramer H (2005) *Drosophila* Vps16A is required for trafficking to lysosomes and biogenesis of pigment granules. *J Cell Sci* **118:** 3663–3673

Ramser J, Abidi FE, Burckle CA, Lenski C, Toriello H, Wen G, Lubs HA, Engert S, Stevenson RE, Meindl A, Schwartz CE, Nguyen G (2005) A unique exonic splice enhancer mutation in a family with X-linked mental retardation and epilepsy points to a novel role of the renin receptor. *Hum Mol Genet* **14:** 1019–1027

Rohrer J, Schweizer A, Russell D, Kornfeld S (1996) The targeting of Lamp1 to lysosomes is dependent on the spacing of its cytoplasmic tail tyrosine sorting motif relative to the membrane. *J Cell* **132:** 565–576

Riediger F, Quack I, Qadri F, Hartleben B, Park JK, Potthoff SA, Sohn D, Sihn G, Rousselle A, Fokuhl V, Maschke U, Purfurst B, Schneider W, Rump LC, Luft FC, Dechend R, Bader M, Huber TB, Nguyen G, Muller DN (2011) Prorenin receptor is essential for podocyte autophagy and survival. *J Am Soc Nephrol* **22:** 2193–2202

Shimada Y, Yonemura S, Ohkura H, Strutt D, Uemura T (2006) Polarized Transport of Frizzled along the Planar Microtubule Arrays in *Drosophila* Wing Epithelium. *Dev Cell* **10:** 209–222

Sihn G, Rousselle A, Vilianovitch L, Burckle C, Bader M (2010) Physiology of the (pro)renin receptor: Wnt of change? *Kidney Int* **78:** 246–256

Simons M, Gloy J, Ganner A, Bullerkotte A, Bashkurov M, Kronig C, Schermer B, Benzing T, Cabello OA, Jenny A, Mlodzik M, Polok B, Driever W, Obara T, Walz G (2005) Inversin, the gene product mutated in nephronophthisis type II, functions as a molecular switch between Wnt signaling pathways. *Nat Genet* **37:** 537–543

Simons M, Mlodzik M (2008) Planar cell polarity signaling: from fly development to human disease. *Annu Rev Genet* **42:** 517–540

Simons M, Walz G (2006) Polycystic kidney disease: cell division without a c(l)ue? *Kidney Int* **70:** 854–864

Storrie B, Desjardins M (1996) The biogenesis of lysosomes: is it a kiss and run, continuous fusion and fission process? *Bioessays* **18:** 895–903

Struhl G, Casal J, Lawrence PA (2012) Dissecting the molecular bridges that mediate the function of Frizzled in planar cell polarity. *Development* **139:** 3665–3674

Strutt DI (2001) Asymmetric localization of frizzled and the establishment of cell polarity in the *Drosophila* wing. *Mol Cell* **7:** 367–375

Strutt H, Strutt D (2008) Differential stability of flamingo protein complexes underlies the establishment of planar polarity. *Curr Biol* **18:** 1555–1564

Strutt H, Warrington SJ, Strutt D (2011) Dynamics of core planar polarity protein turnover and stable assembly into discrete membrane subdomains. *Dev Cell* **20:** 511–525

Usui T, Shima Y, Shimada Y, Hirano S, Burgess RW, Schwarz TL, Takeichi M, Uemura T (1999) Flamingo, a seven-pass transmembrane cadherin, regulates planar cell polarity under the control of Frizzled. *Cell* **98:** 585–595

Vaccari T, Duchi S, Cortese K, Tacchetti C, Bilder D (2010) The vacuolar ATPase is required for physiological as well as pathological activation of the Notch receptor. *Development* **137:** 1825–1832

Veeman MT, Axelrod JD, Moon RT (2003) A second canon. Functions and mechanisms of beta-catenin-independent Wnt signalling. *Dev Cell* **5:** 367–377

Williamson WR, Wang D, Haberman AS, Hiesinger PR (2010) A dual function of V0-ATPase a1 provides an endolysosomal degradation mechanism in *Drosophila* melanogaster photoreceptors. *J Cell Biol* **189:** 885–899

Wu J, Klein TJ, Mlodzik M (2004) Subcellular localization of frizzled receptors, mediated by their cytoplasmic tails, regulates signalling pathway specificity. *PLoS Biol* **2:** E158

Yan Y, Denef N, Schupbach T (2009) The vacuolar proton pump, V-ATPase, is required for notch signalling and endosomal trafficking in *Drosophila*. *Dev Cell* **17:** 387–402